frontiers in Sensors

PERSPECTIVE
published: 21 February 2022
doi: 10.3389/fsens.2021.826403

Towards Real-Time Oxygen Sensing: From Nanomaterials to Plasma

Vinitha Johny[1,2,3†], *K. V. Chinmaya*[1,2,3†], *Muhammed Nihal C. V.*[4], *Varghese Kurian*[1], *G. Mohan Rao*[3,4,5], *Moumita Ghosh*[3,4,5,6] *and Siddharth Ghosh*[1,2,3,7,8,9*]

[1]Department of Science, Open Academic Research Council, Kolkata, India, [2]Department of Science, Open Academic Research UK CIC, Cambridge, United Kingdom, [3]International Center for Nanodevices, Centre for Nano Science and Engineering, Indian Institute of Science, Bengaluru, India, [4]Department of Technology, Open Academic Research Council, Kolkata, India, [5]Department of Technology, Open Academic Research UK CIC, Cambridge, United Kingdom, [6]Advanced Technology Group of FEI Electron Optics, Thermo Fischer Scientific, Eindhoven, Netherlands, [7]Department of Applied Mathematics and Theoretical Physics, University of Cambridge, Cambridge, United Kingdom, [8]Cavendish Laboratory, Maxwell Centre, University of Cambridge, Cambridge, United Kingdom, [9]St John's College, University of Cambridge, Cambridge, United Kingdom

A significantly large scope is available for the scientific and engineering developments of high-throughput ultra-high sensitive oxygen sensors. We give a perspective of oxygen sensing for two physical states of matters—solid-state nanomaterials and plasma. From single-molecule experiments to material selection, we reviewed various aspects of sensing, such as capacitance, photophysics, electron mobility, response time, and a yearly progress. Towards miniaturization, we have highlighted the benefit of lab-on-chip-based devices and showed exemplary measurements of fast real-time oxygen sensing. From the physical–chemistry perspective, plasma holds a strong potential in the application of oxygen sensing. We investigated the current state-of-the-art of electron density, temperature, and design issues of plasma systems. We also show numerical aspects of a low-cost approach towards developing plasma-based oxygen sensor from household candle flame. In this perspective, we give an opinion about a diverse range of scientific insight together, identify the short comings, and open the path for new physical–chemistry device developments of oxygen sensor along with providing a guideline for innovators in oxygen sensing.

Keywords: oxygen sensing, sensors, nanomaterials, plasma, point-care devices, COVID-19

OPEN ACCESS

Edited by:
Gorachand Dutta, Indian Institute of Technology Kharagpur, India

Reviewed by:
Rashidah Arsat, University Technology Malaysia, Malaysia

***Correspondence:**
Siddharth Ghosh
siddharth@openacademicreserach.org

[†]*These authors have contributed equally to this work*

Specialty section:
This article was submitted to Lab-on-a-chip Devices, a section of the journal Frontiers in Sensors

Received: *30 November 2021*
Accepted: *29 December 2021*
Published: *21 February 2022*

Citation:
Johny V, Chinmaya KV, Nihal C. V. M, Kurian V, Rao GM, Ghosh M and Ghosh S (2022) Towards Real-Time Oxygen Sensing: From Nanomaterials to Plasma. Front. Sens. 2:826403. doi: 10.3389/fsens.2021.826403

1 INTRODUCTION

On-site oxygen sensing at the point of care (PoC) is an imperative and timely issue. It is not a trivial problem to solve from the engineering perspective in spite of the well-established fundamental science. The standard of detecting specific elements or molecules with ultra-high sensitivity among various PoC technologies is a continuous debate, which needs to be resolved to address the current demand (Suleman et al. (2021)). Towards resolving them, in this perspective, we communicate our opinion about diverse methods of nanomaterials and plasma for highly sensitive and cost-effective oxygen sensors with an aim towards miniaturization and PoC—**Figure 1.1**.

Severe acute respiratory syndrome (due to COVID-19 or resistant pneumonia or air pollution) is life-threatening and a crisis in the low- and middle-income counties where a few days of oxygen therapy cannot be supplied while diagnostics undergo to determine the root cause (Talwar et al. (2015); Fiji and Howie (2020); Howie et al. (2020)). The motivation for this perspective includes the unavailability of concentrated oxygen and the unreliability of resultant data regarding the

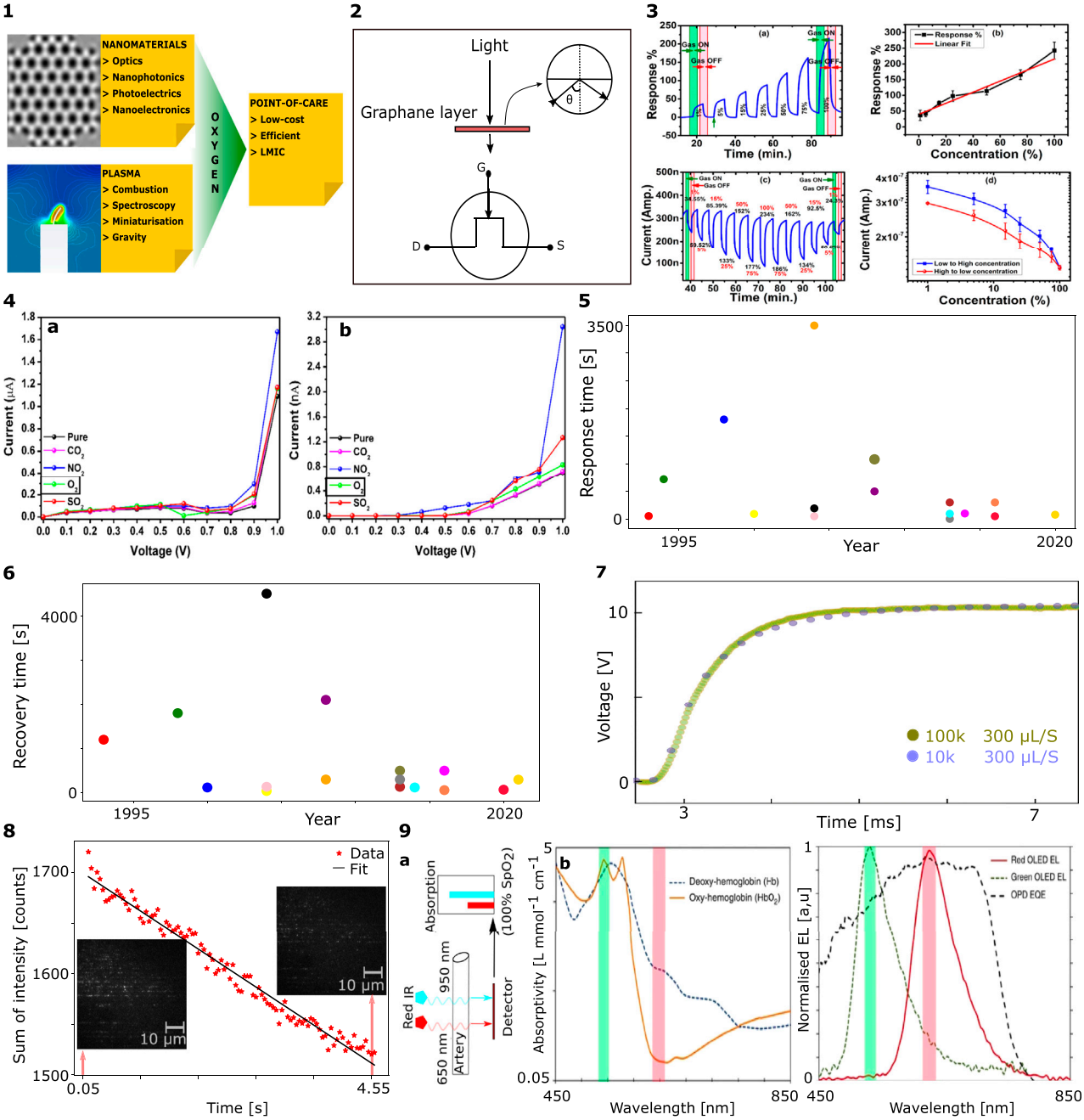

FIGURE 1 | (1) Overview of oxygen sensing with nanomaterials and plasma towards point of care (PoC). **(2)** Principle of graphene-based refractive index sensor. **(3A)** Response of TiS_2 nanomaterials over time with the presence and absence of oxygen gas. **(3B)** Linear response of TiS_2 nanomaterials with respect to the concentration of oxygen gas. Dynamic response of sensor for oxygen and its linear fit. **(3C)** Time-dependent current output from TiS_2 with the presence and absence of oxygen gas. **(3D)** Current output from TiS_2 with respect to concentration of oxygen [adapted from Sakhuja et al. (2020)]. **(4A, 4B)** Current–voltage response of SiBi for oxygen in contrast to other gases along one axis and another axis, respectively [adapted from Kumar et al. (2021)]. **(5)** Ashby plot—progress of material response time for oxygen sensor over the period of 1990 and 2020. **(6)** Ashby plot—progress of material recovery time of nanomaterial-based oxygen sensor with respect to year of published papers. **(7)** Comparison of real-time voltage curve of GRIS at collection frequencies of 10 and 100 kHz [adapted from Xing et al. (2012)]. **(8)** Photooxidation of single Atto-488 fluorphores inside nanofluidic device (inset scale bars = 10 μm). **(9A)** Principle of pulse oximetry sensor with two wavelengths of light. **(9B)** Absorptivity of oxygenated (orange solid line) and deoxygenated (blue dashed line) hemoglobin in arterial blood as a function of wavelength [adapted from Lochner et al. (2014)].

concentration of oxygen level in the blood for medical requirements, which is a continuous problem in other global south countries as well. We could not find an effective low-cost oxygen sensor after performing a significant search in the commercial space (Ahn et al. (2004); Li et al. (2010); Baryeh et al. (2017)). Measuring tools for oxygen levels in the blood and

in the atmosphere should be abundantly available, like clinical thermometers as domestic diagnostic tools and PoC. We investigate the compatibility of existing nanomaterial-based oxygen-sensing mechanisms in PoC applications and their sensitivity and response time in the context of optical and electronics systems. Beyond the solid-state phase of matter, the electrically highly conductive state that is plasma will be indispensable in detecting molecular parameters due to the strong long-range electric and magnetic field interactions. Hence, the latter part of the article discusses the physics of plasma in oxygen sensing. Towards developing single-molecule nanofluidics devices and plasma-based oxygen sensors from a candle flame towards PoC realizations, we show two newly proposed methods.

2 OXYGEN SENSING WITH NANOMATERIALS

2.1 Nanoscale Physical Chemistry

Nanomaterials are famous for various shapes, high surface-to-volume ratios, and non-trivial physics (Cao (2004); Nie et al. (2007); Park et al. (2009); Rao et al. (2009); Sozer and Kokini (2009)), which have been a central attraction since 1959 (Feynman (2018)). The basic principle of oxidation can be applied to engineer low-cost oxygen sensors. Formation of oxides needs to be at a fast rate for immediate response. Besides fast response, fast recovery is also important to design high-throughput oxygen sensors for PoC applications. Refractive index depends on the electronic property of a material, which can be changed due to oxidation. **Figure 1.2** shows the mechanism of optical gating of a transistor to detect change in refractive index due to the presence of oxygen. The overall physical chemistry of nanomaterials is an unavoidable aspect for nanomaterial-based sensors.

2.2 Selection of Nanomaterials

Systematic selection of materials should be the first step towards developing an efficient sensor. To harness a quantitative understanding of material selection for oxygen, let us understand the influencing parameters for oxygen sensing using nanomaterials. They are operating temperatures, structure of material, and electronic properties for better recovery and response time.

Sakhuja et al. (2020) showed room-temperature oxygen detection using liquid exfoliated TiS_2 nanosheet. They observed the TiS_2 nanosheet's dynamic response of oxygen over 90 min with an on–off response time of 10 min as shown in **Figure 1.3A**. The work claims that the response time and recovery are 78 and 70 s, respectively at room temperature. Its dependency on the concentration of oxygen is found to be linear (**Figure 1.3B, C**) and shows current output ranging from 100 to 350 nA with increasing concentrations from 1% to 100% and then decreasing from 100% to 1%. The associated hysteresis error from **Figure 1.3D** was found to be ±3.42%. As a nanomaterial, TiS_2 holds better response and recovery time compared to other materials (Chou et al. (2014); Chaabouni et al. (2004))—ZnO-based sensors require 4,500 s to recover and cannot operate at the entire span of oxygen concentration.

Kumar et al. (2021) demonstrated the use of SiBi-nanosheets for oxygen-containing gas sensing. The current–voltage or I–V characteristics are shown in **Figure 1.4A, B** for different crystal directions. They observed that the adsorption energy of oxygen molecules is −1.10 eV with a work function of 4.22 eV. This finding provides an indication of getting a relatively long recovery time for de-absorbing of oxygen molecules from the SiBi surface. They observed a fast recovery time of 297 s for pure oxygen.

Neri et al. (2005) demonstrated the use of a highly sensitive oxygen sensor based on Pt-doped In_2O_3 nanopowders at 200°C, which showed 60% of sensitivity. Li et al. (2004) used ZnO nanowire transistors for oxygen sensing. These sensors show a fast sensitivity with a recovery time of 47 s at 200 ppm ethanol exposure. Graphene, TiO_2, and zeolite also showed potential material properties to be effective as materials of oxygen sensors based on their sensitivity (Chen et al. (2011); Bai and Zhou (2014); Pan et al. (2017)). Different sample preparation techniques of TiO_2 and doping with different materials open avenue for various innovations in PoC of oxygen sensing (Bai and Zhou (2014)).

Sensitivity of oxygen sensor decreases with an increase in recovery time. However, the response time varies greatly for different nanostructures and their operating condition. In **Figures 1.5 and 1.6**, we use an Ashby plot to present the progress of response time and recovery time of nanomaterials, respectively, in oxygen sensing. The highest response and recovery time of nanomaterial-based oxygen sensing was found in 2020. These advanced nanomaterials with improved sensitivity for oxygen sensing in the air and blood should enable the industry to scale up (Vanderkooi and Wilson (1986); Fidelus et al. (2007); Chong et al. (2020); Wu et al. (2009); Pumera (2010); Ghosal and Sarkar (2018); Katayama et al. (2020); Huynh et al. (2021)). Oxygen can also be detected using several bulk instruments, such as AFM and x-rays to obtain fast results in a limited time. Researchers have used graphane, self-chargeable nano-bio-supercapacitors with microelectronic circuits, to sense oxygen and blood plasma (Kim et al. (2020); Lee et al. (2021)). However, these techniques are limited to rapid PoC applications. One can think of reducing the bulk instruments and using the idea to create oxygen sensors for PoC devices.

2.3 Physics of Sensing Towards Point-of-Care

Single-molecule detection with optics is another avenue towards PoC devices. Fluorescence correlation spectroscopy is an unavoidable method for quantitative determination of molecular oxygen within biological gases and fluids (Opitz et al. (2003)). It cannot be used as PoC devices unless the bulkiness of the optical setup is miniaturized. Optical oxygen sensing can be designed based on the principle of fluorescence bleaching, blinking, or quenching by oxygen (McDonagh et al. (2008)). Optical oxygen sensors depend on the use of a light source, a light detector, and luminescent material that reacts to light. Ground-state oxygen exists in the triplet state and helps in

the easy transition of associated molecules to attain its triplet state, which makes it an efficient quencher. The unpaired spins of oxygen can induce the excited state of the fluorescent molecule to undergo inter-system crossing from the singlet state to the triplet state (Kawaoka et al. (1967); Bergman (1968)).

A perspective of oxygen sensing is unfinished if optical sensors are not discussed as it is exploited significantly to measure the saturation level of oxygen in the blood. Xing et al. (2012) demonstrated that a graphene-based refractive index sensor (GRIS) effectively monitors changes in the local refractive index with a fast response time. The voltage-vs.-time response of the GRIS sensor is shown in **Figure 1.7**. Further research should focus on utilizing these nanomaterials and optics by integrating them with nanophotonics, nanofluidic, and microfluidic devices that imprint the major tool for fast diagnostics and detection of single molecules, viruses, and pathogens as a biosensor (McRae et al. (2015); Yamanaka et al. (2016); Zhang and Misra (2019)). In **Figure 1.8**, we show intensity decay of flowing single fluorophores of Atto-488 excited with 488-nm CW laser inside solid-state nanofluidic channels of 30–100 nm cross-sectional diameter—the line-like structures in the inset suggest single molecules are lining up inside the nanofluidic channels. This intensity decay is due to bleaching over time due to photooxidation. Here, the total intensity counts of fluorophores decays linearly over time, which can be fit with a linear equation of $y = -18.83x + 1.69 \times 10^4$ where y is the sum of intensity and x is time. Within 4.55 s, we acquired significant statistics of this information. Such high-throughput nanofluidic devices for PoC will be a paradigm shift in monitoring oxygen using single molecules (Ghosh et al. (2020)). Lab on chip for these devices has been a key research in upcoming years, which is at a mature stage to be commercialized to designing oxygen sensor devices to study the long-term control and monitoring of chronic and cyclic hypoxia (Grist et al. (2015)).

The ongoing pandemic has generated an unprecedented demand for PoC devices for pulse oximetry. The basic principle of pulse oximetry has been developing since 1876, and it is one of the imperative life-saving innovations till date (von Vierordt (1876); Nicolai (1930); Tremper (1989); Miyasaka et al. (2021)). From the war zone to the intensive care unit, pulse oximetry plays a vital role, and the situation remained unchanged during the COVID-19 pandemic to measure the oxygen saturation level in human blood (Greenhalgh et al. (2021)). Pulse oximetry works on the principle of spectrophotometry by measuring oxygen saturation using two light sources—typically 660 nm (red) and 940 nm (infrared) shown in **Figure 1.9A**. The finding is 145 years old, but it has not yet integrated with 13-year-old smartphone technologies, which uses 2-nm CMOS technology while pulse oximetry still remained primarily bulky and un-calibrated. Lochner et al. (2014) used organic materials for pulse oximeter instead of conventional expensive opto-electronic components (Jubran (1999)). They used green (532 nm) and red (626 nm) organic light-emitting diodes (OLEDs) with an organic photodiode sensitive at the aforementioned wavelengths. These organic optoelectronic pulse oximetry sensors showed oxygenation with 2% error. The electroluminescence of green OLED and red OLED has a Lorentzian response with respect to wavelength and peaks at 500 and 640 nm, respectively. The quantum efficiency of the organic photodiode is over 50% for visible wavelengths and over 98% for ≈640 nm shown in **Figure 1.9B**.

These optoelectronics are inexpensive and have good flexibility that will enable researchers to modify the medical sensors in new shapes and sizes for point-of-care applications. Recently, Pipek et al. (2021) showed the relationship of SpO_2 and heart rates using commercial oximeters and smartwatches in patients with lung diseases. They found a correlation between the results of commercial oximeters and smartwatch devices while evaluating SpO_2 and heart rate measurements. Both devices have negligible statistical differences in the evaluation irrespective of skin color, waist circumference, presence of wrist hair, and enamel nail. There will be certain limitations of false readouts, and patients with hypoxemia who have high arterial oxygen tension levels may not be detected (Ralston et al. (1991); Buckley et al. (1994); Jubran (1999); Greenhalgh et al. (2021)). Today, many new advances in optical oxygen sensors are entering to the market (Michelucci et al. (2019); Browne et al. (2021); Moço and Verkruysse (2021)). However, detailed analyses, calibrations, and modelling should be continued to review the current findings, which will accelerate the dissemination. The different concepts of oxygen sensing can be regarded as a catalyst for developing highly sophisticated oxygen-sensing techniques in the relatively near future.

3 OXYGEN SENSING WITH PLASMA

3.1 Physical Chemistry of Plasma

Plasma science is another sophisticated field coined by Langmuir (1928), but the implementation towards realistic application seems a far-fetched problem, unlike nanomaterials. A pair of electrodes and gases with electrical control systems is the basic requirement to create a controlled plasma. Its shape gives the mean electron density to quantify (or *sense*) the concentration of gases, such as oxygen (**Figure 2.1**). The diffusion and collision of molecular species in a plasma system contribute to its shape and orientation as shown in a candle flame, **Figure 2.2**. Generation of plasma variants is dependent on density, scattering energy, and temperature. Changes in electrode geometry influence plasma generation significantly. Oxygen concentration in a closed system is strongly dependent on the temperature and density of plasma. The Thomson cross-section for scattering of light by electrons ($\sigma_T = 0.665 \times 10^{-29}$ m2) quantifies the radiation emitted from an electron in different directions to identify elemental species. Thus, electron density trajectories (e.g., the solar corona with polynomial expressions) should be a parameter for oxygen sensing in PoC devices. In a candle flame, the intense combustion reactions attribute to its highest temperature region (2200 K) (Zheng et al., 2019) and should provide the amount of available oxygen.

A large number of consistent plasma discharges (like 6.5×10^6) can be produced within a small energy range of 0.006–0.10 J using a "coaxial and parallel-rail" electrode

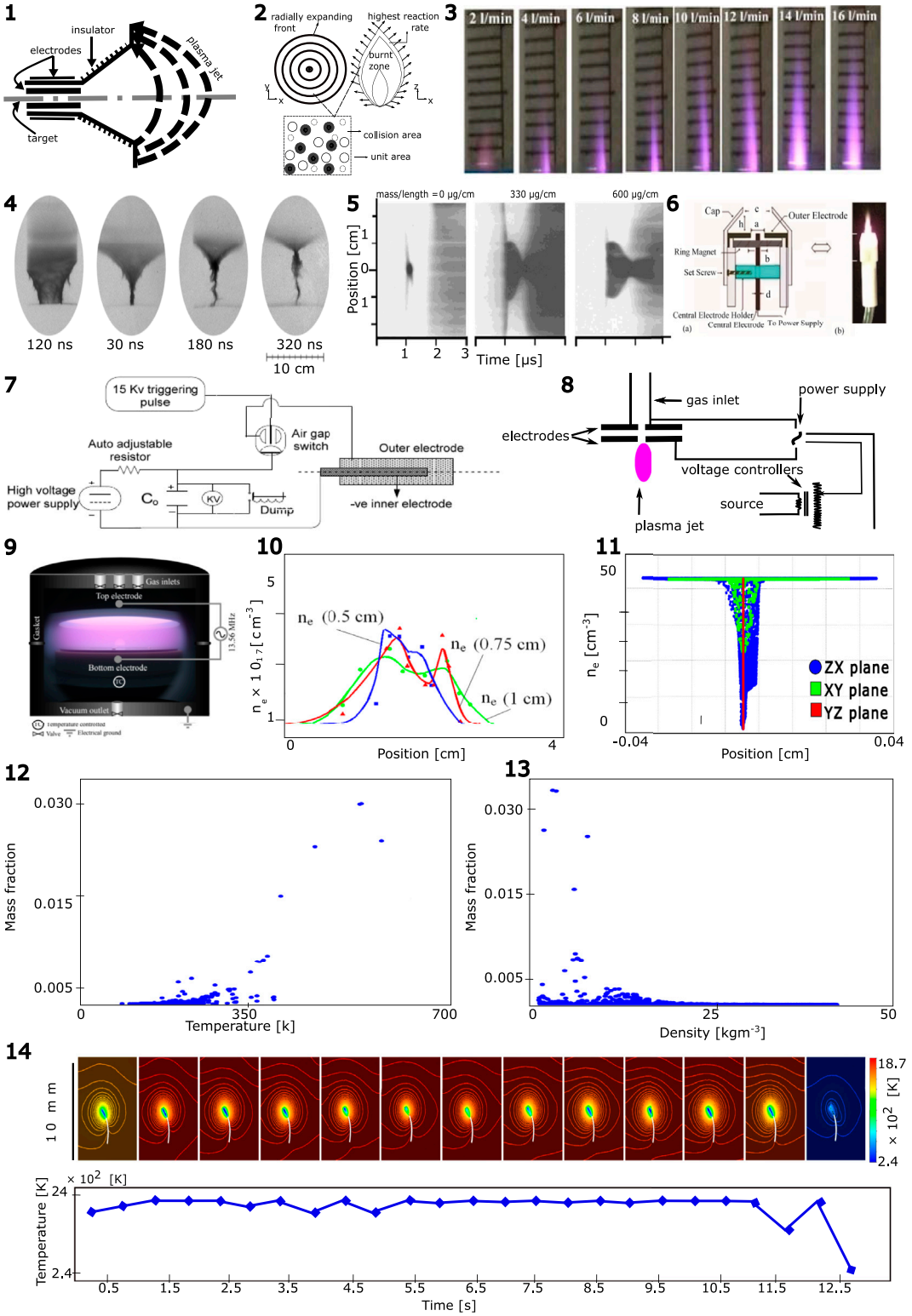

FIGURE 2 | (1) Principle of plasma jet generation. **(2)** Principle of candle flame. **(3)** Plasma length variation with different inlet flow rates [adapted from (Lotfy (2017)]. **(4)** Plasma discharges in pure neon [adapted from Auluck et al. (2021)]. **(5)** The effect of liners in plasma-focusing device (PF) discharge [adapted from Auluck et al. (2021)]. **(6)** An air plasma generation setup [adapted from Kuo (2012)]. **(7)** Circuit design of a 1.5-kJ coaxial plasma device [adapted from Allam et al. (2011)]. **(8)** Electric circuit of nitrogen-plasma jet device [adapted from Lotfy (2017)]. **(9)**, Real-time plasma from an RIE setup [adapted from Ghosh (2016)]. **(10)** Electron density profiles at three different distances from the anode plane [adapted from Auluck et al. (2021)]. **(11)** FEM-simulated electron density vs position of candle flame. **(12)** Temperature-dependent oxygen mass fraction simulation in candle flame. **(13)** Oxygen mass fraction vs density in candle plasma. **(14)** Time-dependent temperature distribution over area of a candle plasma.

geometry (Guman and Peko (1968)). Plasma-focusing devices (PF) operating in the energy range of 10^6–10^7 J (Soto (2005)) should be utilized towards the miniaturization of oxygen sensors. Coupling electrons with plasma instabilities by laser contributes to the effect of magnetic field in plasma temperature and density (Nuckolls et al. (1972)). **Figure 2.3** shows the variation of cold plasma with the inlet flow of N_2 gas in plasma jet device (Lotfy (2017)). It is functional at room temperature and produce reactive oxygen and nitrogen species, thus suitable for wearable applications. At a constant input voltage of 3 kV, a plasma jet length increased initially with the nitrogen flow rate ranging from 2 to 16 l/min until it reached a steady state of 7 mm. **Figure 2.4** [original data shown in Vinogradova et al. (2006)] gives the frame camera pictures from pure neon PF discharge. The purity of air can be found from the emission spectrum of a working gas discharge in air plasma (Anand and Gowravaram (2009)). Another constraint in plasma discharges is liners, as shown in **Figure 2.5** [original data shown in Fortov et al. (2002)]. These highly dense plasma from PF devices acts as a driver for the magnetic compression of liners that can be used for oxygen plasma as well (Fortov et al. (2002)). In a non-equilibrium air plasma produced for medical applications, the emission spectrum corresponding to radiation of 777.4 nm at the plasma plume showed that the plasma flux carried a high concentration of meta-stable atomic oxygen, which extended up to 30 mm from the source (cap)—**Figure 2.6** (Kuo (2012)). An improvised Langmuir probe method with specific electrode geometry gives a 2.5-times higher plasma density (where cathodic electrons ionize the metal to produce electrons and metal ions) and propagation speed (Tian et al. (2019)). The plasma arc diameter varies with different electrode materials. Plasma arc produced between copper electrode and copper work piece at 12 A and 50-μm discharge gap width is found to be 251 μm. Similarly for copper–zinc, copper–steel, steel–steel, and tungsten–steel, it was found to be 300, 233, 270, and 300 μm, respectively, (Li et al. (2020)). The plasma arc with 0.5-mm diameter was measured between copper electrodes with discharge gap width of 0.1 mm and discharge current of 17 A for 80-μs time duration (Kojima et al. (2008)).

3.2 Towards Miniaturization

To construct and design portable plasma systems for PoC, one should investigate large-scale plasma systems. The PF devices are characterized by gas breakdown, formation of current sheath, and its rapid collapse by the action of Lorentz force within a period of few microseconds (Scholz et al. (2000)). Applying this concept, Allam et al. (2011) in **Figure 2.7** studied the orientation and direction of plasma current sheath in a 1.5-kJ coaxial plasma device by the effect of N_2 gas within the pressure range of 1–2.2 Torr. Lotfy (2017) designed and constructed a nitrogen jet plasma device (**Figure 2.8**), which could produce cold plasma extending up to 7 mm from the separation of electrodes. **Figure 2.9** depicts a real-time plasma system under vacuum (Ghosh (2016)). In such an electrically controlled plasma system, the electron density and other fundamental parameters share similar responses. If we go back to PF devices, the electron density distribution with respect to position in a plasma sheath as in **Figure 2.10** [original data shown in Oginov et al. (2004)] has a strong resemblance with the electron density distribution of a candle flame system as shown in **Figure 2.11**. The density slowly rises at the initial stage because of the atomic photoionization and reaches a maximum peak that is around 3×10^{17} cm^{-3} for distances 0.5, 0.75, and 1 cm, from anode plane, and abruptly collapses later. The distribution from a transient simulation of pressure-based turbulence model of a candle flame uses finite element analysis solver (ANSYS Fluent 2021 R1 Stolarski et al. (2018)). This shows miniatured versions of plasma systems for highly sensitive to molecular parameters.

3.3 Parameters of Plasma Systems for Oxygen Sensing

Mass fraction of oxygen sensing-dependent parameters are temperature, electron density, and region of the highest reaction rates. A flat-braid wick candle in an adiabatic enclosure was studied. The time-dependent simulation was carried out for determining the variations in oxygen concentration with time. **Figures 2.12 and 2.13** show the dependence of mass fraction of oxygen on temperature and density, respectively, in our FEM simulation, which has significant similarities with (Cooper (1966)) temperature dependence on the amount of dielectric concentration in plasma. The concentration of oxygen is maximum (at around 650 K temperature) due to incomplete and slow reaction–collision processes involving oxygen. It declines after 650 K due to vigorous reactions at the flame border area in a flame system. As the combustion products increase over time, it pushes away the existing oxygen. The maximum oxygen mass fraction is above 0.030 at around 2 kg/m^3 and approaches a minimum steady value of 0.005 after 10 kg/m^3. Solving the governing rate equations gives the population densities and relaxation times necessary to obtain a steady state in hydrogen plasma (Drawin (1969)). Hence, density is inversely related to the mass fraction of oxygen in the simulated combustion system, which is illustrated in **Figure 2.13**.

3.4 Plasma for Oxygen Sensing

Let us make the path clear towards oxygen sensing from the existing wider perspective. Usually in plasma systems, the radiation loss with time can be estimated from the coronal approximation where the thermal limit is close to the ionization limit (Cooper (1966)). Here, the radiative decay rates are higher compared to the collision decay rates, and the transition probability $A(P)$ from the excited level (P) to the ground level ($P = 1$) will be high. Thus, the excited state of electrons will be short lived and are responsible for the thin optical regime of plasma. In electrical discharge machining, the initial step towards the formation of arc plasma is ionization and breakdown of the dielectric medium, such as oxygen. It was found that the diameter of molten region decreases even though the plasma arc diameter increases. The degree of ionization of a molecular specie depends on the plasma temperature (over 5,000 K) from which the plasma arc area and the rate coefficients for various recombination–collision reactions are estimated (Kojima et al. (2008). In a plasma system, the

molten area is categorized as the region above 1,808 K and the heat-affected area is above 600 K based on the physical changes of electrodes, which confirms the effect of electrode material in plasma diameter (Li et al. (2020)). It also shows variation of dielectric medium, such as oxygen, and its composition alters the plasma arc. The interaction of electrons with electromagnetic waves can vary the refractive index of plasma and determine its electron density (Equipe (1978)).

In our simulated model of a candle flame, the highest temperature is around 2,400 K, which makes the physics of molten region very significant for oxygen sensing. Here, various species collide with air molecules to form the emission spectra (Yambe and Satou (2016)). Thus, comparing and evaluating the molten region before and after the dielectric discharge with respect to the line pair method (Griem (2005)) can be useful for measuring a particular constituent in the system. In a multi-step combustion mechanism with known operating conditions (such as H_2, O_2, HO_2, H^+, OH^-, HO_2, O^{2+}, and δ, which is the third body in our simulation), the concentration of oxygen is found from the rate equations of other species involved in the system Griffiths and Barnard (2019). The candle flame simulation in **Figure 2.14** gives the rate of product emissions and rate of oxygen with time dependency on the species considered for combustion. In more complex burning mechanisms, the mass fraction of various components in the system at a given time can be estimated from the added species and possible products formed. The density of excited states is less than the free electrons and bare nuclei densities, because the relaxation time of excited levels are comparatively small (Bates et al. (1962)), and the energy is generated as radiation when an electron recombines with ionized, atom and this process can be enhanced in the presence of oxygen. In **Figure 2.14**, the emissivity is lower near the wick and increases radially towards the flame border. The flame border is the region of the highest reaction rates, and the emissivity has an inverse relation to wavelength (Zheng et al. (2019)). Plasma-based oxygen sensors can be regarded as an efficient sensing methodology due to its modus operandi and accessibility.

4 DISCUSSION

We found that developments of oxygen-sensing methods from various states of matter are studied with optical, electrical, and chemical means. Oxygen can be determined at the molecular level with single-molecule-level accuracy in real-time at fast timescale. Nanomaterial-based oxygen sensors give accurate measurements on the concentration of molecular oxygen. Lack of safe disposal methods and non-unified policies of hazardous nanomaterial wastes have been a concern. Ranking nanomaterial according to their performance, TiS_2, SiBi, graphene, and zeolite will top the list. The cost of nanomaterial production is decreasing with scalability, but solid-state nanofabrications have been expensive, which needs significant attentions. Plasma-based oxygen sensing is a high-throughput and cost-effective method. It eliminates major organic contaminants and produce less pollutants, but high-energy emissions from plasma should be fine-tuned with energy filters for wearable applications. Giant plasma systems and small confined low-temperature plasma systems share evident similarities in terms of electron density and temperature to the concentration ratio of specific molecular species, which can be adapted for developing oxygen sensors. Candle-based oxygen systems have low-energy emissions, and cold-plasma systems at room-temperature are suitable for wearables. Another cost-effective sensing methodology is solid-state-material-based nanofluidics, which will optimally combine nanomaterials and plasma together to achieve a fast real-time oxygen sensor, which can be analyzed with cutting-edge *in situ* super-resolution microscopy, electron energy loss spectroscopy, and x-ray diffraction. Integrating oxygen concentrator with artificial neural network, lab-on-chip, smartphone technology, and unconventional computing is a way forward to monitor patients with unmanageable health issues, like COVID-19, hypoxia, and resistant pneumonia. Our perspective will give insight to the startups, unicorns, governments, philanthropists, and financial institutions to embark upon creating low-cost oxygen-sensing PoCs for creating a strong health-care-friendly sustainable economy.

DATA AVAILABILITY STATEMENT

The original contributions presented in the study are included in the article/Supplementary Material; further inquiries can be directed to the corresponding author.

AUTHOR CONTRIBUTIONS

VJ and KC collected all the data, analyzed them, and wrote the manuscript. MN and VK performed an extended experiment, which supported the writing of this manuscript. MG, GR, and SG supervised the research and partly wrote the manuscript. SG proposed the research. All authors contributed to the article and approved the submitted version.

FUNDING

The study was supported by the internal funding of the Open Academic Research Council, International Centre for Nanodevices, and the Centre for Nano Science and Engineering, Indian Institute of Science Bangalore.

ACKNOWLEDGMENTS

The authors are thankful to Jintu James, Midhun George Thomas, and Subham Ghosh for productive discussion. All the authors are extremely grateful to Sagar Gosalia for managing the research facilities.

REFERENCES

Ahn, C. H., Choi, J.-W., Beaucage, G., Nevin, J., Lee, J.-B., Puntambekar, A., et al. (2004). Disposable Smart Lab on a Chip for point-of-care Clinical Diagnostics. *Proc. IEEE* 92, 154–173. doi:10.1109/jproc.2003.820548

Allam, T. M., El-Sayed, H. A., and Soliman, H. M. (2011). Plasma Current Sheath Motion in Coaxial Plasma Discharge. *Energ. Power Eng.* 03, 436–443. doi:10.4236/epe.2011.34054

Anand, V., and Gowravaram, M. R. (2009). On the Purity of Atmospheric Glow-Discharge Plasma. *IEEE Trans. Plasma Sci.* 37, 1811–1816. doi:10.1109/TPS.2009.2025949

Auluck, S., Kubes, P., Paduch, M., Sadowski, M. J., Krauz, V. I., Lee, S., et al. (2021). Update on the Scientific Status of the Plasma Focus. *Plasma* 4, 450–669. doi:10.3390/plasma4030033

Bai, J., and Zhou, B. (2014). Titanium Dioxide Nanomaterials for Sensor Applications. *Chem. Rev.* 114, 10131–10176. doi:10.1021/cr400625j

Baryeh, K., Takalkar, S., Lund, M., and Liu, G. (2017). "Introduction to Medical Biosensors for point of Care Applications," in *Medical Biosensors for Point of Care (POC) Applications* (Amsterdam, Netherlands: Elsevier), 3–25. doi:10.1016/b978-0-08-100072-4.00001-0

Bates, D. R., Kingston, A., and McWhirter, R. P. (1962). Recombination between Electrons and Atomic Ions, I. Optically Thin Plasmas. *Proc. R. Soc. Lond. Ser. A. Math. Phys. Sci.* 267, 297–312.

Bergman, I. (1968). Rapid-response Atmospheric Oxygen Monitor Based on Fluorescence Quenching. *Nature* 218, 396. doi:10.1038/218396a0

Browne, S. H., Bernstein, M., and Bickler, P. E. (2021). Accuracy of Smartphone Integrated Pulse Oximetry Meets Full Fda Clearance Standards for Clinical Use. *medRxiv*.

Buckley, R. G., Aks, S. E., Eshom, J. L., Rydman, R., Schaider, J., and Shayne, P. (1994). The Pulse Oximetry gap in Carbon Monoxide Intoxication. *Ann. Emerg. Med.* 24, 252–255. doi:10.1016/s0196-0644(94)70137-7

Cao, G. (2004). *Nanostructures & Nanomaterials: Synthesis, Properties & Applications*. London, United Kingdom: Imperial college press.

Chaabouni, F., Abaab, M., and Rezig, B. (2004). Metrological Characteristics of Zno Oxygen Sensor at Room Temperature. *Sensors Actuators B: Chem.* 100, 200–204. doi:10.1016/j.snb.2003.12.059

Chen, C. W., Hung, S. C., Yang, M. D., Yeh, C. W., Wu, C. H., Chi, G. C., et al. (2011). Oxygen Sensors Made by Monolayer Graphene under Room Temperature. *Appl. Phys. Lett.* 99, 243502. doi:10.1063/1.3668105

Chong, Y., Poschmann, M., Zhang, R., Zhao, S., Hooshmand, M. S., Rothchild, E., et al. (2020). Mechanistic Basis of Oxygen Sensitivity in Titanium. *Sci. Adv.* 6, eabc4060. doi:10.1126/sciadv.abc4060

Chou, C.-S., Wu, Y.-C., and Lin, C.-H. (2014). Oxygen Sensor Utilizing Ultraviolet Irradiation Assisted Zno Nanorods under Low Operation Temperature. *RSC Adv.* 4, 52903–52910. doi:10.1039/c4ra05500d

Cooper, J. (1966). Plasma Spectroscopy. *Rep. Prog. Phys.* 29, 35–130. doi:10.1088/0034-4885/29/1/302

Drawin, H. W. (1969). Influence of Atom-Atom Collisions on the Collisional-Radiative Ionization and Recombination Coefficients of Hydrogen Plasmas. *Z. Physik* 225, 483–493. doi:10.1007/bf01392775

Equipe, T. (1978). Tokamak Plasma Diagnostics. *Nucl. Fusion* 18, 647.

Feynman, R. (2018). "There's Plenty of Room at the Bottom," in *Feynman and Computation* (Boca Raton, Florida, USA: CRC Press), 63–76.

Fidelus, J. D., Łojkowski, W., Millers, D., Grigorjeva, L., Smits, K., and Piticescu, R. R. (2007). Zirconia Based Nanomaterials for Oxygen Sensors - Generation, Characterisation and Optical Properties. *Solid State Phenomena* 128, 141–150. doi:10.4028/www.scientific.net/ssp.128.141

Fiji, C. K., and Howie, S. (2020). The Development and Implementation of an Oxygen Treatment Solution for Health Facilities in Low and Middle-Income Countries. *J. Glob. Health* 10, 020425. doi:10.7189/jgh.10.020425

Fortov, V. E., Karakin, M. A., Khautiev, E. Y., Krauz, V. I., Medovschikov, S. F., Mokeev, A. N., et al. (2002). Study of the Plasma Focus as a Driver for the Magnetic Compression of Liners. *Am. Inst. Phys.* 651, 37–42. doi:10.1063/1.1531276

Ghosal, K., and Sarkar, K. (2018). Biomedical Applications of Graphene Nanomaterials and beyond. *ACS Biomater. Sci. Eng.* 4, 2653–2703. doi:10.1021/acsbiomaterials.8b00376

Ghosh, S., Karedla, N., and Gregor, I. (2020). Single-molecule Confinement with Uniform Electrodynamic Nanofluidics. *Lab. Chip* 20, 3249–3257. doi:10.1039/d0lc00398k

Ghosh, S. (2016). "Nanoscale Photonics: From Single Molecule Nanofluidics to Light-Matter Interaction in Nanostructures,". Ph.D. thesis (Göttingen, Germany: Georg-August-Universität Göttingen).

Greenhalgh, T., Knight, M., Inda-Kim, M., Fulop, N. J., Leach, J., and Vindrola-Padros, C. (2021). Remote Management of Covid-19 Using home Pulse Oximetry and Virtual ward Support. *bmj* 372, n677. doi:10.1136/bmj.n677

Griem, H. R. (2005). *Principles of Plasma Spectroscopy*. Cambridge: Cambridge University Press, 2.

Griffiths, J. F., and Barnard, J. A. (2019). *Flame and Combustion*. Oxfordshire, England, UK: Routledge.

Grist, S., Schmok, J., Liu, M.-C., Chrostowski, L., and Cheung, K. (2015). Designing a Microfluidic Device with Integrated Ratiometric Oxygen Sensors for the Long-Term Control and Monitoring of Chronic and Cyclic Hypoxia. *Sensors* 15, 20030–20052. doi:10.3390/s150820030

Guman, W. J., and Peko, P. E. (1968). Solid-propellant Pulsed Plasma Microthruster Studies. *J. Spacecraft Rockets* 5, 732–733. doi:10.2514/3.29340

Howie, S. R., Ebruke, B. E., Gil, M., Bradley, B., Nyassi, E., Edmonds, T., et al. (2020). The Development and Implementation of an Oxygen Treatment Solution for Health Facilities in Low and Middle-Income Countries. *J. Glob. Health* 10, 020425. doi:10.7189/jgh.10.020425

Huynh, G. T., Kesarwani, V., Walker, J. A., Frith, J. E., Meagher, L., and Corrie, S. R. (2021). Nanomaterials for Reactive Oxygen Species Detection and Monitoring in Biological Environments. *Front. Chem.* 2021, 732.

Jubran, A. (1999). Pulse Oximetry. *Crit. Care* 3, 1–7. doi:10.1186/cc341

Katayama, Y., Fujioka, Y., and Tsukada, K. (2020). Development of a Patch-type Flexible Oxygen Partial Pressure Sensor. *IEEE J. Transl. Eng. Health Med.* 8, 1–7. doi:10.1109/jtehm.2020.3005477

Kawaoka, K., Khan, A. U., and Kearns, D. R. (1967). Role of Singlet Excited States of Molecular Oxygen in the Quenching of Organic Triplet States. *J. Chem. Phys.* 46, 1842–1853. doi:10.1063/1.1840943

Kim, M., Porras-Gomez, M., and Leal, C. (2020). Graphene-based Sensing of Oxygen Transport through Pulmonary Membranes. *Nat. Commun.* 11, 1103–1110. doi:10.1038/s41467-020-14825-9

Kojima, A., Natsu, W., and Kunieda, M. (2008). Spectroscopic Measurement of Arc Plasma Diameter in Edm. *CIRP Ann.* 57, 203–207. doi:10.1016/j.cirp.2008.03.097

Kumar, V., Bano, A., and Roy, D. R. (2021). First-principles Calculations of Sibi Nanosheets as Sensors for Oxygen-Containing Gases. *ACS Appl. Nano Mater.* 4, 2440–2451. doi:10.1021/acsanm.0c02998

Kuo, S. P. (2012). Air Plasma for Medical Applications. *J. Biomed. Sci. Eng.* 5, 61. doi:10.4236/jbise.2012.59061

Langmuir, I. (1928). Oscillations in Ionized Gases. *Proc. Natl. Acad. Sci.* 14, 627–637. doi:10.1073/pnas.14.8.627

Lee, Y., Bandari, V. K., Li, Z., Medina-Sánchez, M., Maitz, M. F., Karnaushenko, D., et al. (2021). Nano-biosupercapacitors Enable Autarkic Sensor Operation in Blood. *Nat. Commun.* 12, 1–10. doi:10.1038/s41467-021-24863-6

Li, C., Shutter, L. A., Wu, P.-M., Ahn, C. H., and Narayan, R. K. (2010). Potential of a Simple Lab-On-A-Tube for point-of-care Measurements of Multiple Analytes. *Lab. Chip* 10, 1476–1479. doi:10.1039/c000897d

Li, Q. H., Liang, Y. X., Wan, Q., and Wang, T. H. (2004). Oxygen Sensing Characteristics of Individual Zno Nanowire Transistors. *Appl. Phys. Lett.* 85, 6389–6391. doi:10.1063/1.1840116

Li, X., Wei, D., Li, Q., and Yang, X. (2020). Study on Effects of Electrode Material and Dielectric Medium on Arc Plasma in Electrical Discharge Machining. *Int. J. Adv. Manuf Technol.* 107, 4403–4413. doi:10.1007/s00170-020-05278-x

Lochner, C. M., Khan, Y., Pierre, A., and Arias, A. C. (2014). All-organic Optoelectronic Sensor for Pulse Oximetry. *Nat. Commun.* 5, 5745–5747. doi:10.1038/ncomms6745

Lotfy, K. (2017). Cold Plasma Jet Construction to Use in Medical, Biology and Polymer Applications. *J. Mod. Phys.* 08, 1901–1910. doi:10.4236/jmp.2017.811113

McDonagh, C., Burke, C. S., and MacCraith, B. D. (2008). Optical Chemical Sensors. *Chem. Rev.* 108, 400–422. doi:10.1021/cr068102g

McRae, M. P., Simmons, G. W., Wong, J., Shadfan, B., Gopalkrishnan, S., Christodoulides, N., et al. (2015). Programmable Bio-Nano-Chip System: a

Flexible point-of-care Platform for Bioscience and Clinical Measurements. *Lab. Chip* 15, 4020–4031. doi:10.1039/c5lc00636h

Michelucci, U., Baumgartner, M., and Venturini, F. (2019). Optical Oxygen Sensing with Artificial Intelligence. *Sensors* 19, 777. doi:10.3390/s19040777

Miyasaka, K., Shelley, K., Takahashi, S., Kubota, H., Ito, K., Yoshiya, I., et al. (2021). Tribute to Dr. Takuo Aoyagi, Inventor of Pulse Oximetry. *J. Anesth.* 2021, 1–39. doi:10.1007/s00540-021-02967-z

Moço, A., and Verkruysse, W. (2021). Pulse Oximetry Based on Photoplethysmography Imaging with Red and green Light. *J. Clin. Monit. Comput.* 35, 123–133. doi:10.1007/s10877-019-00449-y

Neri, G., Bonavita, A., Micali, G., Rizzo, G., Galvagno, S., Niederberger, M., et al. (2005). A Highly Sensitive Oxygen Sensor Operating at Room Temperature Based on Platinum-Doped In2O3 Nanocrystals. *Chem. Commun.* 2005, 6032–6034. doi:10.1039/b510832b

Nicolai, L. (1930). Über Reizstromerzeugung auf lichtelektrischer Grundlage. *Pflügers Arch.* 225, 131–144. doi:10.1007/bf01752109

Nie, S., Xing, Y., Kim, G. J., and Simons, J. W. (2007). Nanotechnology Applications in Cancer. *Annu. Rev. Biomed. Eng.* 9, 257–288. doi:10.1146/annurev.bioeng.9.060906.152025

Nuckolls, J., Wood, L., Thiessen, A., and Zimmerman, G. (1972). Laser Compression of Matter to Super-high Densities: Thermonuclear (Ctr) Applications. *Nature* 239, 139–142. doi:10.1038/239139a0

Oginov, A. V., Karakin, M. A., Krauz, V. I., Myalton, V. V., Valentin, P., Gurey, A. E., et al. (2004). "Study of the dynamics and structure of plasma-current sheath of plasma focus dischar," in *2004 International Conference on High-Power Particle Beams (BEAMS 2004)* (IEEE), 746–749.

Opitz, N., Rothwell, P. J., Oeke, B., and Schwille, P. (2003). Single Molecule Fcs-Based Oxygen Sensor (O2-fcsensor): a New Intrinsically Calibrated Oxygen Sensor Utilizing Fluorescence Correlation Spectroscopy (Fcs) with Single Fluorescent Molecule Detection Sensitivity. *Sensors Actuators B: Chem.* 96, 460–467. doi:10.1016/s0925-4005(03)00601-4

Pan, M., Omar, H., and Rohani, S. (2017). Application of Nanosize Zeolite Molecular Sieves for Medical Oxygen Concentration. *Nanomaterials* 7, 195. doi:10.3390/nano7080195

Park, M.-H., Kim, M. G., Joo, J., Kim, K., Kim, J., Ahn, S., et al. (2009). Silicon Nanotube Battery Anodes. *Nano Lett.* 9, 3844–3847. doi:10.1021/nl902058c

Pipek, L. Z., Nascimento, R. F. V., Acencio, M. M. P., and Teixeira, L. R. (2021). Comparison of Spo2 and Heart Rate Values on Apple Watch and Conventional Commercial Oximeters Devices in Patients with Lung Disease. *Sci. Rep.* 11, 18901–18907. doi:10.1038/s41598-021-98453-3

Pumera, M. (2010). Graphene-based Nanomaterials and Their Electrochemistry. *Chem. Soc. Rev.* 39, 4146–4157. doi:10.1039/c002690p

Ralston, A. C., Webb, R. K., and Runciman, W. B. (1991). Potential Errors in Pulse Oximetry Iii: Effects of Interference, Dyes, Dyshaemoglobins and Other Pigments. *Anaesthesia* 46, 291–295. doi:10.1111/j.1365-2044.1991.tb11501.x

Rao, C. N. R., Sood, A. K., Subrahmanyam, K. S., and Govindaraj, A. (2009). Graphene: the New Two-Dimensional Nanomaterial. *Angew. Chem. Int. Ed.* 48, 7752–7777. doi:10.1002/anie.200901678

Sakhuja, N., Jha, R. K., Chaurasiya, R., Dixit, A., and Bhat, N. (2020). 1t-phase Titanium Disulfide Nanosheets for Sensing H2s and O2. *ACS Appl. Nano Mater.* 3, 3382–3394. doi:10.1021/acsanm.0c00127

Scholz, M., Miklaszewski, R., Gribkov, V., and Mezzetti, F. (2000). Pf-1000 Device. *Nukleonika* 45, 155–158.

Soto, L. (2005). New Trends and Future Perspectives on Plasma Focus Research. *Plasma Phys. Control Fusion* 47, A361–A381. doi:10.1088/0741-3335/47/5a/027

Sozer, N., and Kokini, J. L. (2009). Nanotechnology and its Applications in the Food Sector. *Trends Biotechnology* 27, 82–89. doi:10.1016/j.tibtech.2008.10.010

Stolarski, T., Nakasone, Y., and Yoshimoto, S. (2018). *Engineering Analysis with ANSYS Software*. Oxford, United Kingdom: Butterworth-Heinemann.

Suleman, S., Shukla, S. K., Malhotra, N., Bukkitgar, S. D., Shetti, N. P., Pilloton, R., et al. (2021). Point of Care Detection of Covid-19: Advancement in Biosensing and Diagnostic Methods. *Chem. Eng. J.* 414, 128759. doi:10.1016/j.cej.2021.128759

Talwar, S., Keshri, V. K., Choudhary, S. K., Gupta, S. K., Ramakrishnan, S., Juneja, R., et al. (2015). Surgical Strategies for Patients with Congenital Heart Disease and Severe Pulmonary Hypertension in Low/middle-Income Countries. *Heart Asia* 7, 31–37. doi:10.1136/heartasia-2015-010645

Tian, J., Liu, W., Gao, Y., and Zhao, L. (2019). Discharge and Metallic Plasma Generation Characteristics of an Insulated Anode with a Micropore. *Phys. Plasmas* 26, 023511. doi:10.1063/1.5078677

Tremper, K. K. (1989). Pulse Oximetry. *Chest* 95, 713–715. doi:10.1378/chest.95.4.713

Vanderkooi, J. M., and Wilson, D. F. (1986). "A New Method for Measuring Oxygen Concentration in Biological Systems," in *Oxygen Transport to Tissue VIII* (Berlin, Germany: Springer), 189–193. doi:10.1007/978-1-4684-5188-7_25

Vinogradova, V. P., Karakin, M. A., Krauz, V. I., Mokeev, A. N., Myalton, V. V., Smirnov, V. P., et al. (2006). Dynamics of a High-Temperature Pinch in the Presence of Dust. *Plasma Physics Reports* 32, 642–655.

von Vierordt, K. (1876). *Die quantitative spectralanalyse in ihrer Anwendung auf Physiologie, Physik, Chemie und Technologie*. Tübingen: H. Laupp.

Wu, C., Bull, B., Christensen, K., and McNeill, J. (2009). Ratiometric Single-Nanoparticle Oxygen Sensors for Biological Imaging. *Angew. Chem.* 121, 2779–2783. doi:10.1002/ange.200805894

Xing, F., Liu, Z. B., Deng, Z. C., Kong, X. T., Yan, X. Q., Chen, X. D., et al. (2012). Sensitive Real-Time Monitoring of Refractive Indexes Using a Novel Graphene-Based Optical Sensor. *Sci. Rep.* 2, 908. doi:10.1038/srep00908

Yamanaka, K., Vestergaard, M. d., and Tamiya, E. (2016). Printable Electrochemical Biosensors: a Focus on Screen-Printed Electrodes and Their Application. *Sensors* 16, 1761. doi:10.3390/s16101761

Yambe, K., and Satou, S. (2016). Investigation of Helium Plasma Temperature in Atmospheric-Pressure Plasma Plume Using Line Pair Method. *Phys. Plasmas* 23, 023509. doi:10.1063/1.4942170

Zhang, J., and Misra, R. D. K. (2019). Nanomaterials in Microfluidics for Disease Diagnosis and Therapy Development. *Mater. Technol.* 34, 92–116. doi:10.1080/10667857.2018.1527803

Zheng, S., Ni, L., Liu, H., and Zhou, H. (2019). Measurement of the Distribution of Temperature and Emissivity of a Candle Flame Using Hyperspectral Imaging Technique. *Optik* 183, 222–231. doi:10.1016/j.ijleo.2019.02.077

Conflict of Interest: Author MG is employed by the Thermo Fisher Scientific. Authors VJ and KVC are employed by the International Centre for Nanodevices.

The remaining authors declare that the research was conducted in the absence of any commercial or financial relationships that could be construed as a potential conflict of interest.

Publisher's Note: All claims expressed in this article are solely those of the authors and do not necessarily represent those of their affiliated organizations, or those of the publisher, the editors, and the reviewers. Any product that may be evaluated in this article, or claim that may be made by its manufacturer, is not guaranteed or endorsed by the publisher.